Development of an active sensor module for the RTTOV-SCATT radiative transfer simulator

Rohit Mangla[(1)(2)], Philippe Chambon[(1)], Alan Geer [(3)] and Jayaluxmi Indu[(2)]

(1) : CNRM UMR-3589, Météo-France & CNRS, Toulouse, France
(2) : Indian Institute of Technology, Bombay, India
(3) : ECMWF, Reading, United Kingdom

Correspondence to philippe.chambon@meteo.fr

1. Introduction

Active microwave sensors are becoming widely used observations within the Numerical Weather Prediction community, either for validating model forecasts or for assimilation purposes. Just as in the forward simulation of passive microwave observations, it is necessary to make assumptions on the scattering properties of hydrometeors. With the objective of simulating both active and passive microwave instruments within a single framework using the same radiative transfer assumptions in a widely-used tool in the NWP community, an active sensor module is currently under development within the RTTOV-SCATT V12 software (Saunders et al., 2018). This module will support the GPM/DPR instrument as well as the Cloudsat/CPR instrument. In the work presented below, simulations based on the ARPEGE global model running operationally at Météo-France are shown. Statistical comparisons are made between observations and simulations considering several radiative properties assumptions of the snow. Theses simulations results are used to assess the quality of the cloud forecasts of two ARPEGE simulations with two different convection schemes.

The ARPEGE global model

The **ARPEGE model** is the global model in operations at Météo-France. It is characterized by a horizontal stretched and tilted grid as shown on Figure 1. The table below presents a few characteristics of the version in operations and of the versions used in the present study :

	ARPEGE	ARPEGE in this study	
	in operations	Research version	Research version
Horizontal resol./Nb levels	T1800 / 105 levels	T1200 / 105 levels	T1200 / 105 levels
Deep conv.	Bougeault et al. scheme	Bougeault et al. scheme	Tiedtke et al. scheme
DAS	4D-Var 6h cycles	4D-Var 6h cycles	4D-Var 6h cycles
Forecasts	+102h	+102h	+102h

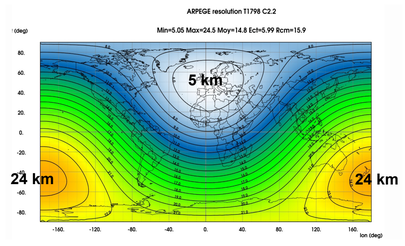

Figure 1: ARPEGE stretched and tilted grid at T1800 truncature

Active microwave sensors for clouds and precipitation

GPM Dual-frequency Precipitation Radar

On board the Global Precipitation Measurement Core satellite.

	KuPR	KaPR
Freq. (GHz)	**13.6**	**35.5**
Hori. resol. (km)	5	5
Swath width (km)	245	120

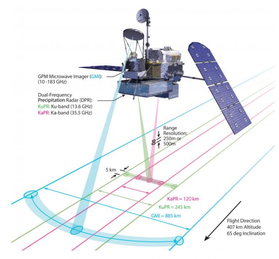

Figure2: Illustration of Dual-frequency Precipitation Radar (© NASA)

Cloudsat Cloud Profiling Radar

On board the Cloudsat satellite

94 GHz frequency

Nadir-viewing

Horizontal resolution:
1.2 km cross-track
3.5 km along-track

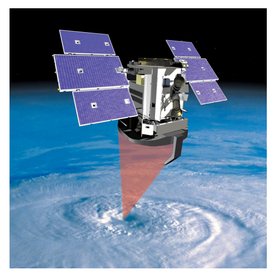

Figure3: Illustration of the Cloud Profiling Radar (© NASA).

2. Simulating radar reflectivities with the RTTOV-SCATT software

The RTTOV-SCATT software is a widely used tool among NWP centres to simulate microwave observations and is equipped with all the necessary features to build up a simple space-radar simulator, benefiting from all the developments implemented for passive microwave observations like DDA-based Single Scattering Properties (SSP) (Geer and Baordo, 2014).

In the present study, the following SSP and Particle Size Distributions (PSD) are used for the simulation of reflectivities with a modified version of the RTTOV-SCATT V12 software:

- Rainfall: SSP => Mie sphere ; PSD => Marshall-Palmer distribution
- Cloud Ice and Cloud Water: SSP => Mie sphere PSD => Modified Gamma distribution
- Snow particle: SSP => the 15 new particle shapes available within RTTOV 12 represented on Figure 4 (Eriksson et al., 2018) + the 9 particle shapes from the Liu database PSD => Field et al. 2007 in tropical regime.

The simulated reflectivities shown in this study take into account the attenuation from both hydrometeors and gases.

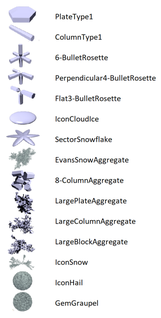

Figure 4: 15 particles from Eriksson et al. (2018) available in RTTOV-SCATT V12

3. Taking into account cloud and precipitation fraction profiles within the simulations

Within the RTTOV-SCATT software, the simulation of passive microwave brightness temperatures is performed using a two column approach. The final simulated TB is a weighed combination of a clear column TB and a cloudy column TB. The weighing factor (*cfrac)*, can either be prescribed by the user or computed internally using a combination of the cloud cover profile and the hydrometeors profiles. This *cfrac* factor is also used for normalizing the hydrometeor contents and deriving the hydrometeor contents of the cloudy column. Below one compare reflectivity simulations with two different calculations: (i) using a single cloud "cfrac" fraction applying to the whole profile and all hydrometeors using the formula shown below, (ii) using a "hydrofrac" which provides a dedicated profile of fractions for each hydrometeor type. Those fraction are used twice, first dividing to compute the in-cloud hydrometeor amount, then multiplying to compute the total reflectivity across clear and cloudy columns.

A 3-layer cloudy situation with no large scale precipitation in between the highest cloud and the midlevel cloud

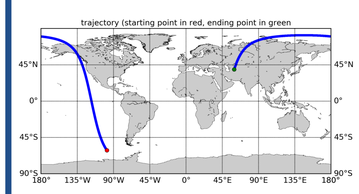

Figure 5: Ground track of one orbit of Cloudsat for May 1st 2018. The red dot corresponds to the beginning of the orbit file and the green dot to the end of it.

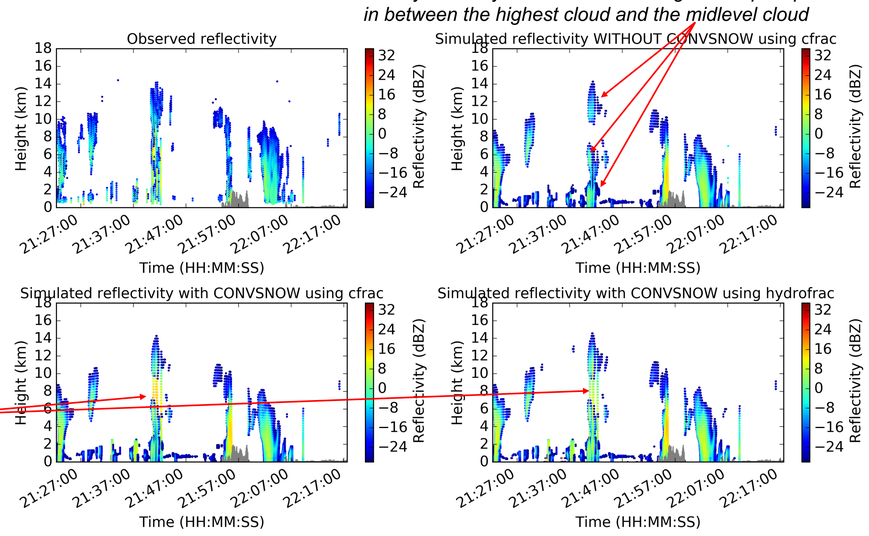

Figure 6: Observed reflectivities for the orbit shown on Figure 5 (top left). RTTOV-SCATT simulations with the ARPEGE forecast at 3h lead time initialised on May 1st 18h UTC. The top right simulation does include only large scale hydrometeors, the bottom left simulations include both large scale and convective hydrometeors with a normalisation by cfrac. The Bottom right simulation simulation include both large scale and convective hydrometeors with a normalisation by profiles of cloud and precipitation fractions.

Normalizing the hydrometeor contents by either cfrac or a dedicated hydrometeor fraction lead to very different reflectivities. In this case, the simulation with cfrac seems to overestimate the observed reflectivities

In this example, the default cfrac is diagnosed to roughly 0.44

$$cfrac = \frac{\sum_{level} Hydrometeors\ Content * Cloud\ cover}{\sum_{level} Hydrometeor\ Content}$$

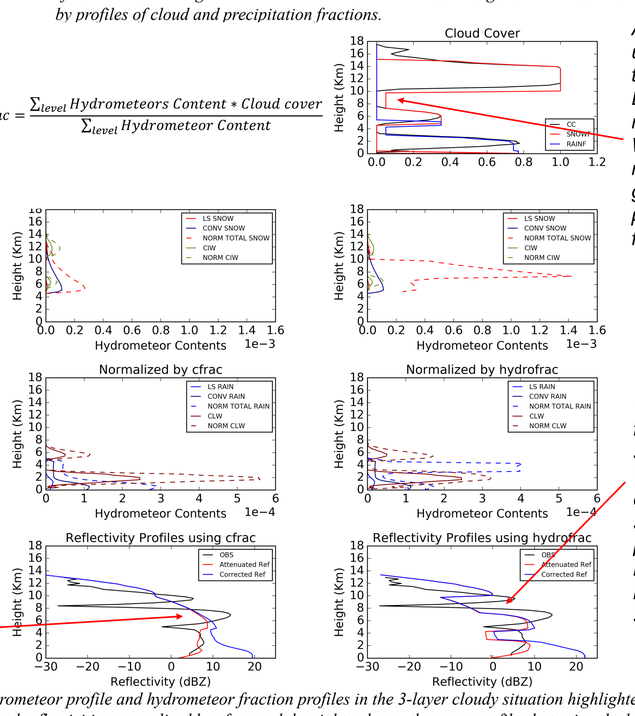

As for the precipitation fraction used, a diagnostic is used from the cloud cover profile as in the ECMWF model and shown in red for snow and blue for rain. When only convective snow or rain is present in the column at a given level, a fraction of 5% is prescribed as hydrometeor fraction

With the dedicated hydrometeor fraction profiles, layers can ben seen in the simulated profile. While not perfect as it is showing discontinuities related to the too strong discontinuity of precipitation fraction, the use of hydrometeor fraction does improve the realism of the simulation

In the observed profile, the 3 layers can be seen but in the simulations with the cfrac normalization factor, the layers are not simulated because of the overestimation of the convective snow fraction

Figure 7: Example of hydrometeor profile and hydrometeor fraction profiles in the 3-layer cloudy situation highlighted above. The left column shows the hydrometeors and reflectivities normalized by cfrac and the right column, the same profiles but using the hydrometeor fractions.

Simulations over a full-month of data have been performed with the cfrac normalization and normalization of hydrometeors with dedicated fraction profiles. It was found that the simulations using hydrofractions are closer to the observations (not shown), it is therefore this configuration which is used in the rest of the poster.

4. Comparing observed and simulated reflectivities taking into account the observation operator uncertainties

RTTOV-SCATT simulations of Cloudsat reflectivities have been performed from 11th May to 10th June 2018 with ARPEGE 3h forecasts using the Bougeault convection scheme, and compared to Cloudsat observed reflectivities. For each atmospheric column of the model collocated with one observation, 26 forward simulations have been performed, corresponding to the 26 particle shapes available within the Liu and the *Eriksson et al.* databases.

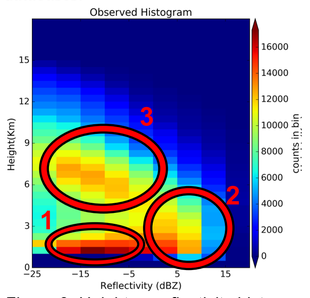

Figure 8: Height vs reflectivity histogram of observations over oceans for the month of May, 2018. Following Marchand et al. (2009), the circles correspond to the occurrence of:
(1): nondrizzling boundary layer clouds
(2): drizzle and rain
(3): precipitating ice

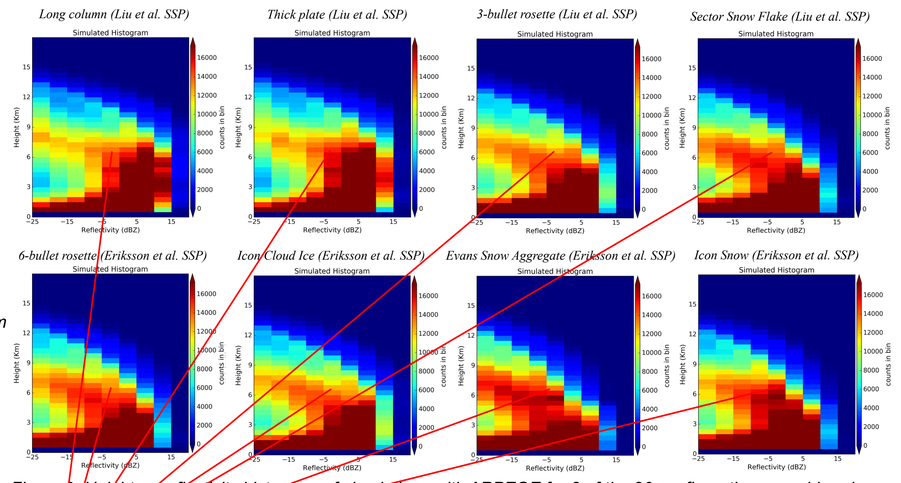

Figure 9: Height vs reflectivity histogram of simulations with ARPEGE for 8 of the 26 configurations considered.

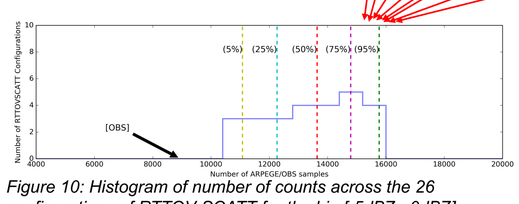

Figure 10: Histogram of number of counts across the 26 configurations of RTTOV-SCATT for the bin [-5dBZ ; 0dBZ] [6.5km ; 7km]

The histogram of simulations varying quite significantly with the particle shape considered for the single scattering properties of snow, we define below a simple method to extract only the conclusions of comparisons which are quite robust to the observation operator uncertainties:

(i) For each bin of height and reflectivity, we compute percentiles values from the 26 values of count in the bin :5%, 25%, 50%, 75%, 95% (Having only 26 scenarios is rather limited and it is likely the percentiles would be better defined with more simulations)

(ii) The number of counts of the histogram of observations is compared to the percentiles value. The bin of height and reflectivity is then categorized in the diagram shown below.

From this comparison, one can see that the ARPEGE simulations with the Bougeault convection scheme do overestimated the occurrence of nondrizzling boundary layer clouds as well as drizzle and rain. Conclusions for precipitating ice are more mixed depending on the height.

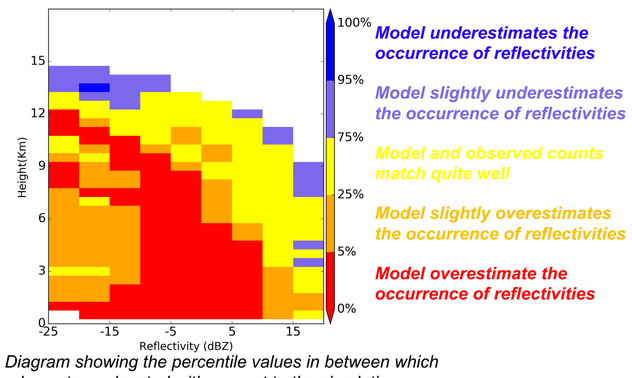

Figure 11: Diagram showing the percentile values in between which the observed counts are located with respect to the simulations

5. Comparing ARPEGE simulations with two different convection schemes

The same simulations as above have been performed for ARPEGE forecasts using the Tiedtke convection scheme. The same diagnostics as in Figure 11 is presented in Figure 12 for these additional runs.

Overall, an improvement can be seen with the Tiedtke scheme compared to the Bougeault scheme, with more "yellow" bins indicating less overestimation of occurrence of precipitating ice and well as boundary layer clouds.

Figure 12: Same as Figure 11

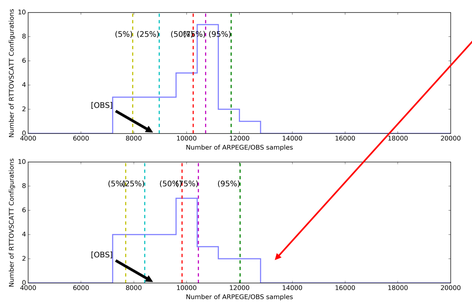

Figure 13: Histogram of number of counts across the 26 configurations of RTTOV-SCATT for the bin [-20dBZ ; -15dBZ] [2.5km ; 3km]. The top histogram corresponds to ARPEGE forecasts with the Bougeault scheme and the bottom histogram to ARPEGE forecasts with the Tiedtke scheme.

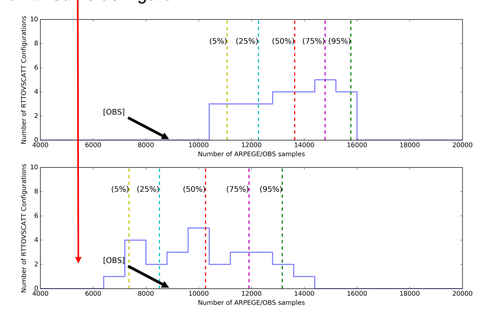

Figure 14: Histogram of number of counts across the 26 configurations of RTTOV-SCATT for the bin [-5dBZ ; 0dBZ] [6.5km ; 7km]. The top histogram corresponds to ARPEGE forecasts with the Bougeault scheme and the bottom histogram to ARPEGE forecasts with the Tiedtke scheme.

6. Conclusion and perspectives

In this work, simulations of reflectivities with the RTTOV-SCATT forward operator have been performed for the ARPEGE global model. The differences of simulated reflectivities between taking into account a single *cfrac* index and hydrometeor fraction profiles in the normalization of hydrometeor content have been shown on a case study. Then histograms of height versus reflectivities have been computed over a one month period. The observed and simulated histograms have been compared using a simple method taking into account uncertainties related to the observation operator. It was shown that ARPEGE simulations with the Tiedtke convection scheme are characterized by a better agreement with the Cloudsat observations.

Future work include applying the same methodology to GPM/DPR simulations. This capability of the RTTOV-SCATT to simulated active instruments will be included in a future version of RTTOV (likely Version 13).

Saunders, R., Hocking, J., Turner, E., Rayer, P., Rundle, D., Brunel, P., ... & Bormann, N. (2018). An update on the RTTOV fast radiative transfer model (currently at version 12). Geoscientific Model Development, 11(7), 2717-2737.
Eriksson, P., Ekelund, R., Mendrok, J., Brath, M., Lemke, O., and Buehler, S. A.: A general database of hydrometeor single scattering properties at microwave and sub-millimetre wavelengths, Earth Syst. Sci. Data, 10, 1301-1326, https://doi.org/10.5194/essd-10-1301-2018, 2018.
Marchand, R., Haynes, J., Mace, G. G., Ackerman, T., and Stephens, G. (2009), A comparison of simulated cloud radar output from the multiscale modeling framework global climate model with CloudSat cloud radar observations, *J. Geophys. Res.*, 114, D00A20, doi:10.1029/2008JD009790.

The authors are grateful to Sara Q. Zhang and Mary Borderies for fruitful discussions which helped developing this framework. Rohit Mangla was funded by the Raman Charpak fellowship through the Indo-French Centre for the Promotion of Advanced Research (IFCPAR/CEFIPRA).